

# Technical implications of land monitoring projects using remote sensing data in Central America for natural resources management

Sandra Bolaños<sup>1</sup>, Thomas Oberthur<sup>2</sup>

International Center for Tropical Agriculture (CIAT)  
AA 6713, Cali, Colombia

<sup>1</sup>s.bolanos@cgiar.org, <sup>2</sup>t.oberthur@cgiar.org

**Abstract – The monitoring of changes in types of land cover has been of great importance to evaluate the impacts in soil degradation and the availability of water for agriculture. In this study this change has been translated in spatial patterns of land use and the results have been taken to a GIS with the intention of analyzing their dynamics.**

**The general purpose of this paper is to reveal technical implications of radiometric and geometric calibrations in our methodology used to detect land use/land cover changes for a period of 15 years, and demonstrate its impact in the final accuracy. The final objective is to quantify the change in a small catchment of the Calico River in Nicaragua, in order to give information reliable for use in the evaluation and analysis of the actual condition of the natural resources and for use in predictive models, such as landslide modelling.**

**Keywords:** land cover change, radiometric calibration, geometric calibration, agriculture, DEM.

## 1. INTRODUCTION

Due to the historical development of remote sensing platforms and technology, reconstructing land cover changes in a subwatershed over periods greater than fifteen years requires multiple sources of information [Hyman, 2002]. The scarcity of information at higher scales and the lack of standardization of historical maps produce several problems in the use of past sources of information. The lack of information at scales higher than 1:500000 and high spatial resolution imagery, such as aerial photos, or images without clouds in tropical areas, has forced us to study the dynamics based only on data available, comparable and accurate at a mid-range resolution, using Landsat images from 1984 to 2000. The analyst needs to make a product that will reduce problems for making assessments in the future.

In this project, we use change detection techniques in order to monitor land use dynamics, agricultural trends and the landscape evolution in one of CIAT's main hot spots for agricultural development. Understanding land cover change processes improves our capacity to develop sustainable agricultural systems.

How can we compare remote sensing information taken in multiple dates and different atmospheric conditions?  
How can we characterize agroecosystems (pastures and annual crops) and their dynamics from remote sensing images?

Our experience with this project in Central America shows that efforts to analyze land cover change for agricultural applications hinge on the problem of scale in discriminating annual crops from vegetation, and compare them using traditional methods from remote sensing. For example, when the chlorophyll activity is strong, and under similar water content and temperatures in the wet season, all types of vegetation (pastures, crops and forest) appear equal. We could not use textural information in this season at this scale, in order to discriminate crops from other vegetation with Landsat images.

Our paper describes a land cover change analysis in the small catchment in Nicaragua, taken from 1984 to 2000. We discuss several remote sensing techniques based on our case study, and we discuss the difficulties of integrating data from different dates and sensors (TM4 and TM5) in order to see the dynamics of the agricultural border. Then, we discuss what can be done in future studies to prevent many of the problems we experienced in geometric and radiometric calibration of the images.

## 2. LAND COVER CHANGE MAPPING: THE TRADITIONAL METHODOLOGY

Researchers at the International Center for Tropical Agriculture (CIAT) and other research centers commonly analyze land cover change using a traditional method of georeferencing and thematic mapping for each image in the group. The georeferencing is commonly developed with ground control points (GCPs) between image and vector or geocoded image. In this case, the geometric model is calculated for each image based on polynomial equation that involves only the geographic and pixel/line coordinates causing some matching problems between images even when the Root Mean Square Error (RMSE) be less than half a pixel.

The land cover change mapping uses a process that involves post-comparison analysis of land use maps from each image. The classification process for each image uses a supervised classification with field or visual sampling, and cluster analysis to sampling evaluation, to obtain a contingency or separability values that mean good or wrong samples. If the evaluation results have fitted the requirements the samples are introduced into supervised classification algorithm (maximum likelihood or minimum distance) which gives to each pixel, a class value. Another traditional approach is the manual digitizing of class polygons using visual interpretation, matching color palette in a particular a band combination [Puig, 2000]

Finally, land cover maps are compared using a spatial analysis algorithm, which quantifies the area for each coverage, and, under the same area to compare land cover pixels.. This overlapping process try to monitor increase or decrease of land cover types. But sometimes, his methodology gives imprecise results when the landscape units had changed, for example, when river change after a natural disaster, such as flooding, landslides or erosion.

### 3. LAND COVER CHANGE MAPPING: OUR METHODOLOGY

#### 3.1 Geometric Correction and Orthorectification

The geometric correction methodology used in this project, make use of the viewing geometry by satellite orbital parameters and GCPs. The geometric model obtained for each image is link to geometric model of others image by the same GCPs [Toutin, 1997] Ground control points in one image "link" this image to terrain coordinates, but GCps in two or more images link the images to terrain, and make a link between images. For the robust model, one point which link one or two images is good, but one point that link two or more images is better [Toutin, 1997]. The RMSE obtained with 11 images was 0.8 pixels, about 100 GCP per image. When the orbital information was not found into image file, it was get from Internet, or adapted from other image with the same sensor. The images would be orthorectified using the final geometric model and a Digital Elevation Model. Because of the lack of appropriate terrain modeling for this area, we generated a DEM from aerial photos using automatized photogrammetric techniques.

#### 3.2 DEM generation and editing

Using high precision GCPs taken at roads with a Leica 200 GPS System, and aerial photographs at 1:40.000 scale, we produced the DEM, with 10m of pixel spacing. The RMSE for this DEM was 0.47 pixels.

The algorithm calculates the elevation measuring the parallax between corresponding points in each stereo-pair. The automatic detection of corresponding points uses the radiometric correlation between one pixel and its neighbors in a moving window. The point is found when the correlation is maximum between the windows in the right and left images. The software makes the segmentation using a blocks technique for locating corresponding points. The GCPs for DEM generation were collected in double monoscopy.

The altitudes in the DEM are on the top of the vegetation, because it's the pixel representation of the terrain. If the altitudes on the soil are required, a manual correction in a 3D stereo plotter is necessary. For this reason, there were some erroneous pixels in the final DEM. . Because high accuracy was not necessary at our scale, we decided to apply a spatial filter in order to remove these erroneous pixels instead of manual correction.

There are common spatial filters for this correction (i.e., average, medium, etc.) but they modify not only the wrong pixels but also correct neighboring pixels, modifying all data in

the DEM. So, an additional effort is necessary to detect the wrong pixels and to separate them from the rest of the pixels in the DEM. We found that calculating a focal function in GIS software using the standard deviation of a moving window, is possible to discriminate these "peaks" and "sinks" that are present in a photogrammetric DEM. You can correct the sinks using hydrologic modelling also. Using a mask with the upper standard deviation of 20m, we use an average filter to edit the DEM only under this mask, and keep the rest of pixel values as they were.

In order to verify the matching between DEM and the georeferenced image we looked for planimetric features in the DEM. Using hydrological modeling we derive the rivers and microcatchment boundaries, and we use them as a key features. We also use field GCP points to evaluate the images and assess the DEM accuracy in X, Y, Z.

#### 3.3 Topographic Normalization

The image orthorectification doesn't eliminate the terrain shadows. It only corrects the pixel position with respect to relief displacement, but not its value. In order to eliminate terrain shadows and artificial brightness present in the pixels that are in the slopes facing the sensor, we tried to apply common algorithm for topographic normalization. This uses a lambertian reflectance model, orbit information (to calculate elevation angle and solar azimuth), and model illumination conditions, giving us maximum and minimum illumination values for each pixel. Multiplying this value by the digital number of pixels it makes the correction to the image. The results correct some shadows on the terrain, but also introduce wrong brightness in others. So, as a topographic normalization factor, we use the Normalized Difference Vegetation Index.

For the areas with steep topography and very shallow image elevation angles, the topographic normalization is practically impossible, even using a vegetation index. This is because the angle of incidence is more than 90 degrees, meaning there is only diffuse radiance, and no incident radiance, reducing the spectral range for land covers in the image.

#### 3.4 Atmospheric Correction

Haze effects modify the spectral response at the top of the atmosphere. It means that the images have more brightness than they have in clear areas, confusing the land cover types. We test two methods for this correction. First we apply a high point spread algorithm available in ERDAS?, but it produces fine landscape fragmentation, causing a textural change. The second method applies a histogram adjust using pseudo invariant points, orbital information, solar elevation angle, julian day, theoretical gain and bias for each band and theoretical solar spectral irradiance. It is based on the fact that the atmosphere has additive, diffusion and attenuation effects, which makes the histogram a narrow bell shape (Beaulieu, 2002). Taking the "clearest" image as a reference, and pseudoinvariant points from clear water, bare soil and forest we calculate the reflectance adjusted as we can see in Fig 1.

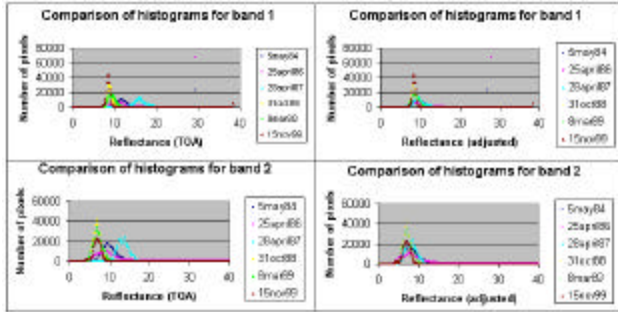


Figure 1. Adjusted reflectance for images

If the reflectance is estimated for reference image, we can calculate an equivalent reflectance for the rest of the images, making a relative calibration also. If the evaluation of the visible bands of the histogram doesn't show a significant narrowing of the haze image with respect to reference image, there is no multiplicative effect, and just an additive correction using from points on clear water is enough. If we appreciate a change in the histogram bands of red and Infrared, this corresponds to land cover changes. But even if the images are calibrated with respect to a reference image, the reflectance values are affected by water content, making the calibration inappropriate.

### 3.5 Radiometric Calibration

Two methodologies were applied for radiometric calibration of the images. First of them was the relative calibration of images with pseudoinvariant points (Furby, 2001). In this case, for relative correction it is assumed that the digital levels in one image are related to the reference image by linear equation using a multiplicative factor (gain) and additive factor (offset). It is assumed that at least 50% of the points are invariant on the scene; give us a confidence factor when part of the pseudoinvariant points change, without affect the calibration coefficients estimated. As in the atmospheric correction, it is required to eliminate non-linear effects over the scene.

Taking into account that the field sampling was made on 2002, we choose the 2000 image as a reference image. Some pseudoinvariant points on clear water, bare soil and urban features were selected on the images and used for calculate the coefficients in a least-square regression. The model was refined iteratively and two final models with weighted least-square calibration lines and weighted least-square calibration with break point were obtained. An evaluation of the histogram of the calibrated images was made as we can see in Fig.2. Some other points were chosen in order to compare the digital values, before and after calibration. The covariance level was from 67% to 93% and weighted least-square regression with break point gave the best matching between calibrated images and reference image.

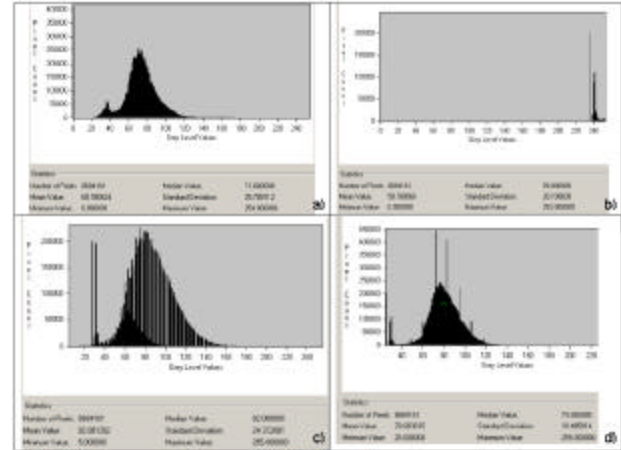


Figure 2. Comparison between histograms of the a) reference image b) 1997 image c) 1997 image calibrated with linear regression d) 1997 image calibrated with least-square regression and break point

In spite of this methodology seems working very well, when we use the calibrated images for classification, the reference signatures don't work very well. To emphasize, the pseudoinvariant points are chosen by visual inspection, introducing errors in little differences.

The second methodology uses pseudoinvariant points chosen in the spectral space (Young Du & Chilar, 2002), based on multitemporal principal components Analysis (PCA) of a set of images. The scatterplot for the same band of multitemporal composition of the same area, its assumed to be on a straight line with a slope value of 1 if there are not linear effects or land cover changes. If the images have linear effects without land cover change, the straight line, has a slope upper than 1. If there are some land cover changes, the digital levels of the images, are not aligned, but the principal axes of the cluster, should have a slope of 1 if the images doesn't have linear effects between them. The eigen values of the principal component 1 in a multitemporal composition of band 1 of date a, and band 1 of date 2, give us the slope of the line of correlation. All PCA had taken 2000 image as a reference. The results are showed in Table 1. Areas with water and clouds were removed because they introduce non-linear effects in the correlation of the images.

	2000-1997	2000-1989	2000-1987	2000-1984
Band 1	0.959	0.681	0.829	0.495
Band 2	0.986	0.932	0.964	0.965
Band 3	0.987	0.896	0.942	0.932
Band 4	0.662	0.636	0.432	0.522
Band 5	0.938	0.740	0.817	0.573
Band 7	0.978	0.868	0.924	0.787

Table 1: Eigen values of Principal Components Analysis on multitemporal composition.

The calculation of new digital levels of the images, uses a linear equation with gain and bias, but here gain is the relationship between the standard deviation of pseudoinvariant points in the images and offset its calculated using the relationship between maximum mean and standard deviation, in order to preserve gain?1 and offset?0. The success of this

methodology is to have a slope of 0.95 in the PCA, and, as is showed in the table 1 the PCA slope for many images are far from this value, reason to consider this method not applicable.

### 3.6 Sampling evaluation and Classification

In our case, it was not possible to calibrate the radiometry between images, and the reasons could be the difference in time and environmental conditions when each image was taken. We had to use field sampling to the classification, with a previous visual inspection of each sample in order to evaluate the accuracy of the survey. We started the classification process with 2000 image, and evaluating the separability, we tried to identify clusters that can be used to build the spectral signatures.

Taking the spectral bands we couldn't separate the signatures of certain land cover classes such as maize and pastures, and looking for better separability in this similar classes, we apply some spectral enhancements as multispectral Principal Component Analysis and Tasseled Cap Transformation. The behavior between first and second component for maize and pastures was much better to discriminate than the several combinations of the original bands or others transformations. Fig. 3. Shows the separability in a feature space spectral plot.

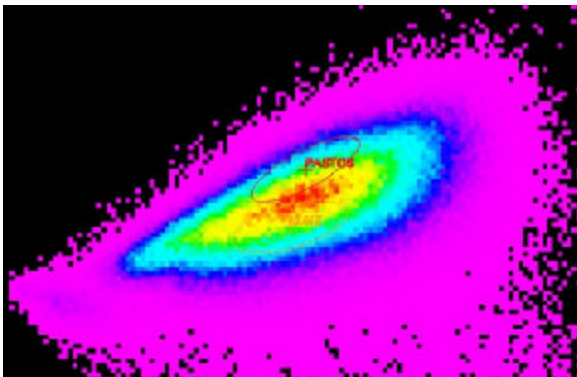


Figure 3. Spectral Plots of Principal components 1 and 2 for land cover discrimination.

#### 4. DISCUSSION: ISSUES UNIQUE TO LAND COVER CHANGE ANALYSIS

Traditional georeferencing methodologies with separate geometric models for each image in a set for land cover change analysis are not useful to make a comparison pixel by pixel. A more robust geometric model that includes the geometry of viewing is necessary.

The radiometric calibration, when the images are taken in a difference of time of 15 years, or with different geometric viewing or soil moisture conditions, are really difficult and imprecise, if the purpose is to make an spectral comparison of the values. The atmospheric correction using trial and error to match the histograms can be some tedious when you have more images, and pseudoinvariant points are not very clear.

In this study, we use 3-band composition for each date, using PC1, PC2 and Normalized Difference Vegetation Index to

correct the topographic effects over the digital levels (shadows and brightness) and to get the forest and clouds class, sometimes confusing with the PC. The principal components 1 and 2 discriminate the classes of interest, and they correct the atmospheric noise, eliminating the redundant information.

#### 5. RESULTS: LAND COVER CHANGE ANALYSIS

Final land cover maps were evaluated, and the overall accuracy shows a general tendency to increase with the difference in radiometry between the each image, and the reference image.

	1984	1987	1989	1993	1997	2000
% Accuracy	86.00	93.00	91	96	89	94

Table 2. Overall Accuracy of the classification

The classification accuracy for each land cover type was assessed, finding a decrease in maize and pastures, for all images.

Land Cover	1984	1987	1989	1993	1997	2000
Forest / coffee under forest	96.57	95.83	96.36	95.00	88.46	100
Pastures	93.33	75.00	84.61	93.75	91.66	93.02
Maize	69.23	83.00	83.18	71.43	81.23	82.35
Shrubland / coffee without forest	90.00	77.3	75.00	71.43	80.00	80.00
Bare Soil	100.00	80.00	100.00	100.00	87.33	83.33
Clouds	95.24	100	N/A	91.67	N/A	97.5
Shadows		87.3	N/A	100	N/A	100.00
Barren or Sparsely Vegetated	90.63	90.00	93.75	100.00	91.67	100.00

Table 3. Accuracy for each coverage, in multiple dates

#### 6. REFERENCES

- Beaulieu, N. Rule-based image processing techniques to monitor environmental dynamics in support to local planning. Internal Report, CIAT July 2002
- Furby, S. L. and Campbell N.A. (2001). Calibrating images from different dates to 'like value' digital counts. Remote Sensing of Environment No 77 pp186-196
- Toutin, Th. Generation of DEM from Stereo Images with a Photogrammetric Approach: Examples with VIR and SAR Data. CCRS database publications 1995.
- Hyman, G. Puig, J. Bolanos, S. (2002). Multisource remote sensing and GIS for exploring deforestation patterns and processes in the Central Peruvian Amazon, 29<sup>th</sup> Symposium of Remote Sensing for Environment
- Puig, J; Leclerc, G. and H. Eva. 2000. Metodologia para Analisis Multitemporal de Areas con Procesos de Deforestacion. Estudio de Casos en America Latina con el Proyecto TREES. IX Simposio Latinoamericano de Percepción Remota. Puerto Iguazú, Argentina
- Yong Du, Philippe M. Teillet and Josef Chilar, Radiometric normalization of multitemporal high-resolution satellite images with quality control for land cover change detection, Remote Sensing of Environment Volume 82 (1): 123-134, September 2002